Effect of Doped Oxides on Cathode Erosion in Nitrogen Free Burning Arc

Y. Takemoto, M. Tanaka and T. Watanabe

Department of Chemical Engineering, Kyushu University, Fukuoka, Japan

Abstract: Nitrogen DC arcs are applied to economical nanoparticle synthesis. However, large electrode erosion is a problem. Electrode temperature and arc temperature were successfully measured synchronously in 50vol%N_2-Ar DC plasma to clarify the electrode erosion mechanism. Electrode shape during erosion can be classified into three categories corresponding to the metal oxide doped in the cathode; rim formation, protrusion formation, and no-shape change. This study improves the quality of nanoparticle with nitrogen DC arcs.

Keywords: thermal plasma, high-speed visualization, electrode temperature, arc temperature

1. Introduction

DC arcs have been applied to the synthesis of metal nanoparticles because of their high temperatures above 10,000 K, high chemical activity, and rapid cooling capability. One of the important issues for DC arcs is to reduce cathode erosion. The reduction of cathode erosion enables stable operation of the process for long periods of time and prevents contamination of the product with electrode-derived substances. Conventionally, an electrode consisting of W, a metal with a high melting point, and a metal oxide with a low work function added by several wt% is used as a cathode to improve arc stability and reduce cathode erosion [1].

Nitrogen has been attracting attention as an inexpensive atmospheric gas. However, electrode wear worsens under nitrogen atmosphere [2]. Metal contamination due to electrode wear causes quality degradation in nanoparticle synthesis.

Temperature measurement of thermal plasmas have been conducted to investigate plasma characteristics. Conventionally, optical spectroscopic techniques were widely used to measure the temperature distribution of thermal plasmas. From the spectroscopic data, arc temperature can be determined by several methods, such as the Fowler-Milne method [3], and the Boltzmann plot method [4]. However, time-resolved information cannot be obtained due to the long acquisition time.

Imaging technique based on high-speed camera observation with band-pass filters has been developed to solve this problem. Temperature distribution of free-burning arc was successfully visualized [5]. However, the relatively low spectral resolution of the high-speed camera system leads to measurement temperature errors. In this study, both line and continuum emissions were considered to solve the problem of high-speed camera imaging technique.

Research about temperature measurement of N_2 DC arc have been published in the past few decades. However, the understanding about the effect of rare earth metal oxide on arc temperature in N_2 atmosphere is insufficient. The purpose of this study was to reveal the cathode erosion mechanism of DC arcs in a nitrogen atmosphere. To investigate the effect of doped oxide, arc temperature and cathode temperature were performed synchronously with two high-speed cameras and four band-pass filters.

2. Temperature Measurement Principle

2.1. Arc Temperature Measurement Method

Arc temperature distribution was calculated from the relationship between relative intensity and temperature. Band-pass filters of 480±5 nm and 500±5 nm were selected for use in temperature measurement. These filters mainly transmit the line spectrum of single charged Ar ion or N ion.

The theoretical emission coefficient through a band-pass filter was calculated as a function of temperature under the assumption of local thermal equilibrium and optically thin. The contribution from line emissions (bound-bound, bb) and two types of continuum radiation, bremsstrahlung emission (free-free, ff) and recombination radiation (free-bound, fb) were included in the calculation. **Figure 1** shows an example of the calculation result. The theoretical emission intensity ratio was calculated from theoretical emission coefficients in two different wavelength regions.

Figure 2 shows the theoretical curves when only the line spectrum was considered and when both the line and continuum emissions were considered. The accuracy of the measured temperature improves by about 1,000 K at 20,000 K when continuum emissions were considered.

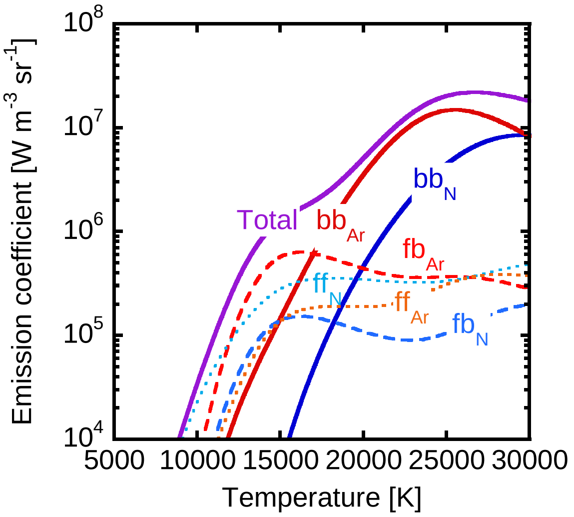

Fig. 1. Temperature dependence of emission coefficients in 50vol%N_2-Ar arc with the BPF of 480±5 nm. bb: line emission, fb: recombination radiation, ff: bremsstrahlung emission.

2.2. Cathode Temperature Measurement Method

Two-color radiation thermometry was performed for electrode temperature measurements [2]. Band-pass filters at 785±2.5 nm and 882±5 nm were chosen to avoid arc-derived line spectra

3. Experimental Setup

Figure 3 is schematic illustration of DC arc plasma system. Water-cooled copper plate was set as the anode. W-2wt%ThO_2, W-2wt%Y_2O_3, W-2wt%La_2O_3 and W-2wt%Ce_2O_3 were used as the cathodes. Cathode diameters was 6 mm. The electrode gap distance was 10 mm. Arc current was 200 A. Gas composition was 50vol%N_2-Ar.

Synchronized measurements of two high-speed cameras were taken to calculate arc and electrode temperatures. In the calculation of arc temperature, Abel inversion was performed [6].

4. Results and Discussion

Figure 4 shows high-speed snaps captured at 1, 5, and 10 min after arc ignition. These images were observed through band-pass filter at 785 nm. Electrode shape during erosion can be classified into three categories. A rim forms in first pattern as observed in W-2wt%ThO_2. Protrusions are formed at the tip of the cathode as the cathode wears out in the second pattern such as W-2wt%La_2O_3 and W-2wt%Ce_2O_3. The shape of the electrode is not significantly changed in the last pattern as in W-2wt%Y_2O_3. The cathode shape does not change significantly at least on a 10-min time scale in argon atmosphere [7]. The first and second patterns of cathode erosion are caused by the presence of nitrogen in the plasma gas.

Figure 5 shows high-speed camera snapshots of electrodes observed through band-pass filter at 785 nm and the corresponding electrode temperature distributions estimated by two-color radiation thermometry. The tip temperature of all metal oxide-doped cathode was about 3,700 K at 1 min after arc ignition. W-2wt%ThO_2 formed a temperature field exceeding 3,600 K at the tip of the electrode below the rim. The temperature distribution of W-2wt%Y_2O_3 was almost unchanged. Protrusions formed at the tip of the electrode in the W-2wt%La_2O_3. The temperature at the tip exceeded 4,500 K. W-2wt%Ce_2O_3 deformed the tip of the electrode into a convex shape. The tip temperature decreased with time. For the electrodes of W-2wt%La_2O_3 and W-2wt%Ce_2O_3, locally higher electrode temperatures were calculated in the low brightness region due to reflected light from the arc.

Figure 6 shows high-speed camera snapshots of arc observed through band-pass filter at 480 nm and the corresponding arc temperature distributions estimated by intensity ratio method with consideration of continuum and line emissions. W-2wt%ThO_2 had the highest arc temperature at about 27,000 K. Conversely, W-2wt%Y_2O_3 had the lowest maximum arc temperature of approximately 25,000 K.

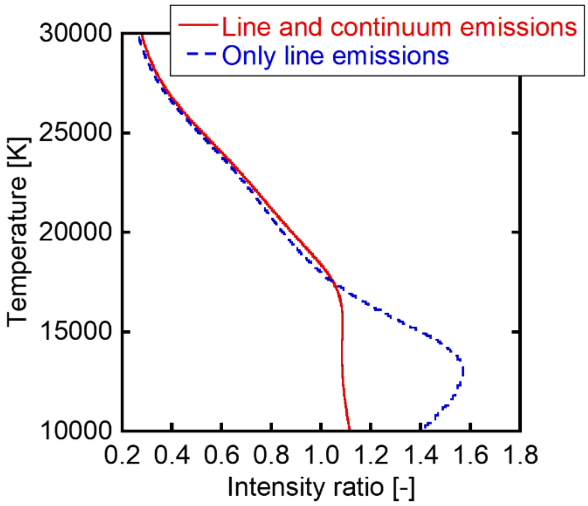

Fig. 2. Relationship between relative intensity and temperature for BPFs combination of 480±5 nm and 500±5 nm in 50vol%N_2-Ar.

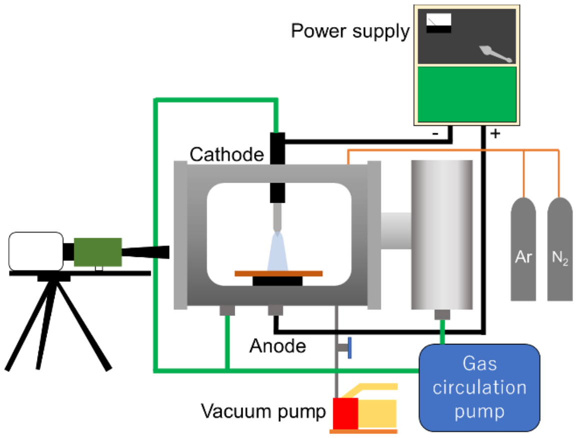

Fig. 3. Schematic diagram of DC arc system.

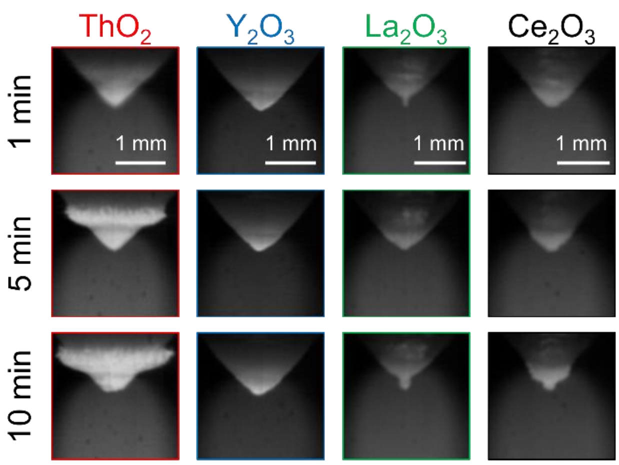

Fig. 4. Image of cathode measured at 785 nm wavelength at 1, 5 and 10 min after ignition.

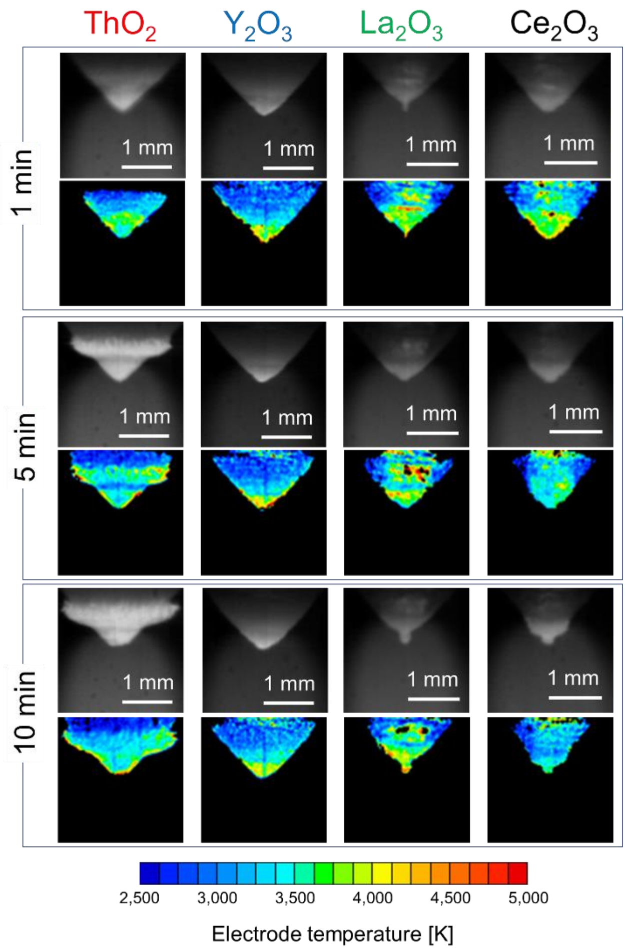

Fig. 6. High-speed snapshots of electrode and corresponding electrode temperature distributions at 1, 5, 10 min after ignition.

Rim has been observed experimentally in high-current argon atmospheres [8]. This indicates that a rim can form due to the increased heat load on the electrode. **Table 1** shows the properties of metal oxides and tungsten. ThO_2 has a small difference in melting point from tungsten compared to other metal oxides. Widely covering the surface of a non-molten tungsten electrode with molten ThO2 is difficult. Local heating occurs when nitrogen recombines on the cathode surface. W-2wt%ThO_2 was greatly affected by the local heating and a rim was formed.

The local heating may also affect the evaporation of metal oxides. The temperature at the tip of the W-2wt%La_2O_3 was higher than 4,500 K. This temperature is above the boiling point of La_2O_3. The evaporation of the metal oxide was accelerated at the tip of the electrode, resulting in the formation of protrusions at the tip of the electrode.

Reactions between nitrogen and electrodes may occur in a nitrogen atmosphere. **Figure 7** shows the Gibbs free energy for the reaction of a nitrogen radical with a metal oxide. Gibbs energy change becomes negative at temperatures above 3,700 K for Ce_2O_3 and 3,900 K for

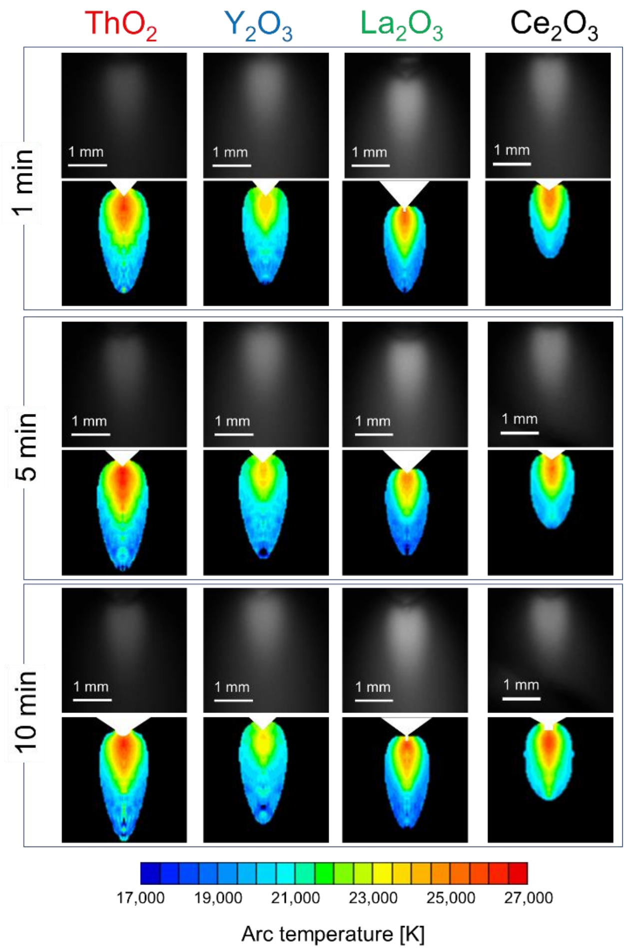

Fig. 5. High-speed snapshots of arc and corresponding arc temperature distributions at 1, 5, 10 min after ignition.

La_2O_3. La_2O_3 and Ce_2O_3 are decomposed at the electrode tip by reaction with nitrogen radicals. The metal oxide is

Table 1. Properties of metal oxides and tungsten.

Emitter	Melting Point [K]	Boiling Point [K]	Work Function [eV]
W	3,695	5,828	4.5
ThO_2	3,323	4,673	2.6
Y_2O_3	2,712	4,563	2.0
La_2O_3	2,577	4,473	3.1
Ce_2O_3	2,483	4,003	3.2

decomposed by reaction with nitrogen radicals at the tip of the electrode, and a protrusion is formed.

5. Conclusion

The effect of metal oxides doped in tungsten electrodes on the wear of tungsten electrodes was investigated in a nitrogen atmosphere. Visualization of electrode temperature distributions and arc temperature distributions was successfully achieved by the synchronization of two high-speed cameras with four bandpass filters of different wavelengths.

Electrode shape during erosion can be classified into three categories. The rim was formed in the first type. The protrusion was formed at the tip of the electrode in the second type. The shape does not change in the last type. The first and second patterns of electrode erosion were not confirmed under argon conditions at the same current value. The first type is caused by the nitrogen recombination heat on the surface of the cathode with the addition of a high melting point metal oxide. The second type is caused by the consumption of metal oxides at the electrode tip by evaporation or reaction with nitrogen radicals.

6. Acknowledgements

This work was supported by JST SPRING, Grant Number JPMJSP2136.

7. References

[1] A. A. Sadek, et al., Metallurgical and Materials Transactions A, **21**, 12, 3221-3236 (1990).
[2] N. Sakura, et al., Japanese Journal of Applied Physics, **59**, 116001 (2020).
[3] R. H. Fowler and E. A. Mine, Monthly Notices of the Royal Astronomical Society, **83**, 7, 403-424 (1923).
[4] K. Hiraoka, et al., Welding International, **11**, 9, 688-696 (1997).
[5] B. Bachmann, et al., Journal of Physics D: Applied Physics, **46**, 125203 (2013).
[6] O. H. Nestor and H. N. Olsen, SIAM Review, **2**, 3, 200-207 (1960).
[7] M. Ushio, et al., Plasma Chemistry and Plasma Processing, **11**, 1, 81-101 (1991).
[8] K. Tanaka, et al., Quarterly Journal of the Japan Welding Society, **13**, 4, 524-531 (1995).

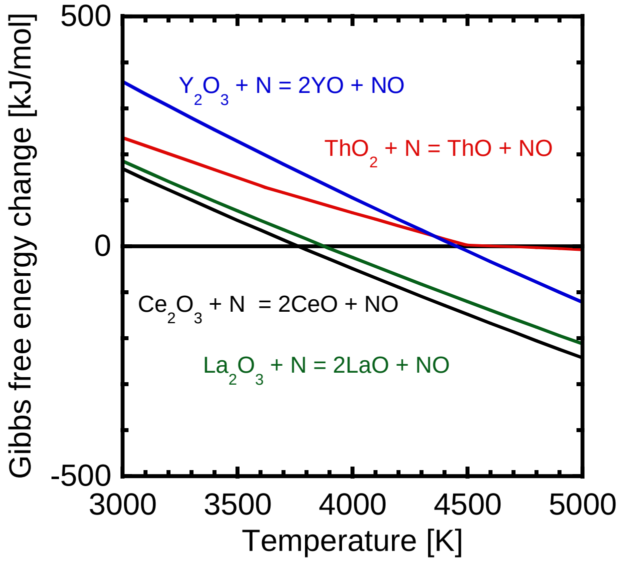

Fig. 7. Gibbs free energy for the reaction of a nitrogen radical with a metal oxide.